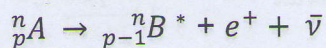
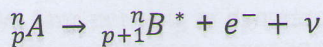


0. Basics and Devices/Materials used

0.1 β -Decay and γ -Radiation

When a radioactive nucleus disintegrates it decays into an excited daughter nucleus with a neutron transforming into a proton by emitting an electron and a neutrino (β^- - decay) or with a neutron turning into a proton by emitting a positron and an antineutrino (β^+ - decay):



The excited nucleus may either relax by emitting a γ -quant or by transferring the excess energy to a shell electron which can result in the emission of a characteristic x-ray or the ionization of the atom. Electrons that received energy in this way are called **conversion electrons**.

0.2 Interaction of γ -Radiation with matter

In General the intensity of γ -Radiation will fall exponentially when entering matter because of various forms of interactions. The decay of intensity is described by the Beer-Lambert law:

$$I = I_0 e^{-\mu x}$$

With x being the level of penetration and μ being the absorbtion coefficient. Normally it is preferred using the so-called mass absorbtion coefficient $\frac{\mu}{\rho}$ when trying to compare the absorbtion properties of different materials as we can take into account irregularities in the density ρ of the absorber material.

There are three main ways in which γ -Radiation can interact with matter: The **Photoeffect**, The **Compton-Effect (Compton-Scattering)** and **Pair Production**.

0.2.1 The Photoeffect:

When entering the surface area of a material a γ -quant can transfer its whole energy to an inner shell electron of the absorber material causing it to be freed, ionizing the absorbing atom. The resulting hole can be recombined by emission of characteristic X-rays or can cause further ionizing of the atom by emitting another electron (Auger-effect). Both the freed atom and any recombination radiation can be detected, making it possible to measure the whole energy of the incident γ -quant.

0.2.2 The Compton-Effect:

A γ -quant can interact with an almost free electron, causing it to be inelastically scattered by transferring part of its energy to the electron, causing the wavelength λ of the γ -quant to be reduced.

The change in the wavelength depends on the scattering angle in the following way:

$$\Delta\lambda = \lambda_c(1 - \cos\theta)$$

$$\lambda_c = \frac{h}{m_e c} : \text{Compton wavelength} \quad \theta : \text{Scattering angle}$$

As the γ -quants wavelength is directly related to its energy we can see that the Compton-Effect gives rise to a continuous energy spectrum (**Compton Plateau**)

$$E' = E - \frac{E}{1 + \frac{E}{m_e \cdot c^2} (1 - \cos \vartheta)}$$

with a sharp edge at a scattering angle of 180° which is called the **Compton edge**

$$E_{Max}' = E - \frac{E}{1 + \frac{2E}{m_e \cdot c^2}}$$

with E being the original energy of the γ -quant.

The Compton Effect can also occur in the Isolation material used during the experiment which causes the detector to detect backscattered γ -quants at an energy of

$$E_{Backscatter} = \frac{E}{1 + \frac{2E}{m_e \cdot c^2}}$$

The line in the spectrum that appears due to this effect is referred to as **Backscatter Line**.

0.2.3 The Pair Production:

When a γ -quant enters the electrical field of a nucleus and possesses energy that exceeds 1,022 MeV (twice the rest mass of an electron/positron) by a small amount Pair Production is possible.

The γ -quant will turn into an electron-positron pair with its energy being converted into rest mass energy of the 2 created particles and kinetic energy:

$$E_\gamma = 2m_e \cdot c^2 + E_{Kin}^e + E_{Kin}^{e^+}$$

If the pair production occurs inside of the detector the positron may recombine with an electron in the detector material causing two γ -quants at an energy of $m_e \cdot c^2 = 511\text{keV}$ each to be emitted. If one or both of the γ -quants escape undetected the detector will register energy peaks at reduced energies.

These peaks are called **single escape line** (at $E_\gamma - 511\text{keV}$) and **double escape line**

(at $E_\gamma - 1022\text{keV}$). If Pair Production occurs outside of the detector, γ -quants emitted by the annihilation process of an electron and a positron may be detected giving rise to the **annihilation line** (at 511keV) in the spectrum.

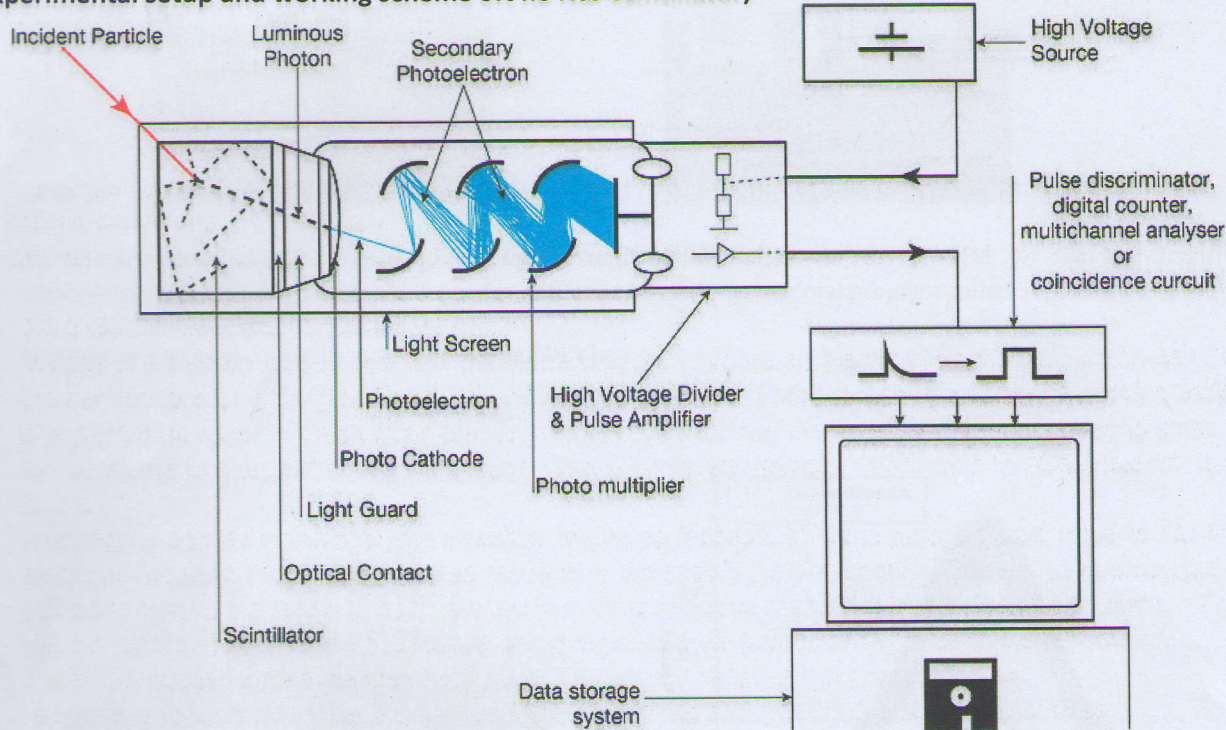
0.3 Detectors:

In this experiment we make use of two different detectors:
A NaI-Scintillator and a Ge semiconductor detector.

0.3.1 NaJ-scintillator:

In the scintillator detector the NaI-crystal is struck by γ -photons. Due to the photo- and compton effect, primary electrons are being created, which excite the atoms in the crystal by ionizing them creating secondary electrons in the process and causing them to emit weak light flashes. These light flashes knock electrons out of a photo cathode and therefore produce a current which can be amplified by a secondary electron multiplier (SEM), that consists of dynodes. An electric field then accelerates the electrons, which causes emission of more and more secondary electrons after each dynode from the dynode material.

Experimental setup and working scheme of the NaI-Scintillator)



This picture represents our experimental setup (only difference being that we also used an oscilloscope). The setup was basically the same for the Ge-Detector

Source: http://en.wikipedia.org/wiki/File:Scintillation_Counter_Schematic.jpg

0.3.2 Ge-Semiconductor-Detector

In case of a semiconductor detector, the incident photon excites an electron into the conduction-band of the semiconductor leaving behind a hole in the valence-band. This process is the inverse of the creation of a photon by recombination of an electrons-hole pair. Normally the detector must be cooled to small temperatures to ensure that the conduction band is completely empty. In principle the GeLidetector is a diode.

A voltage is applied in the opposite direction, the holes (acceptors) in the p-doped area move to - and the electrons (donors) in the n-doped area move to +, increasing the p-n junction. The e-h pairs produced in this zone disturb the recombination current in a more sensitive manner than outside of the junction. Thus the p-n junction is where the quants are being registered via a disturbance pulse in the recombination current, produced by the electron hole pairs. The energy necessary for producing an e-h pair is about 3 eV for Ge. So a 1 MeV photon creates about 330000 electrons and holes.

For both detectors we use a multichannel-analyzer that sorts and counts the pulses by energy into channels by order of magnitude to give out via a software. (MAESTRO)

0.4 Materials and Devices used

Nal-Scintillator

Ge-Semiconductor-Detector

High voltage power supply

Main amplifier

Oscilloscope

Multichannel Analyzer with Interface to a PC and analyzing software (MAESTRO)

Various radioactive sources (Cs137, Co60, Na22, Am241, Ba133)

Various plates of absorber materials lead, copper and aluminium with varying thicknesses (between 2 and 3mm)

Single plates of unknown thickness of Sn, Sb, Te and J

1. Experiment and Results

1.1 Calibration of the NaJ-Scintillator

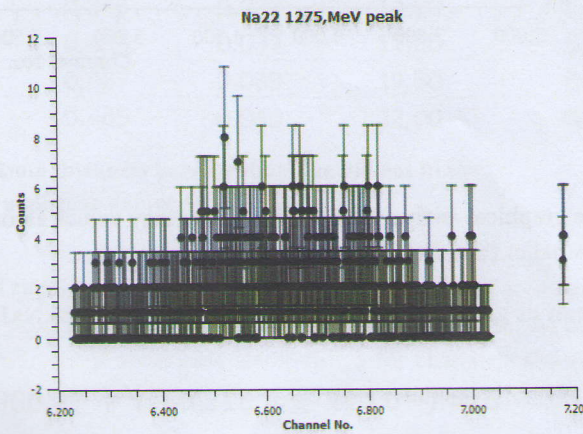
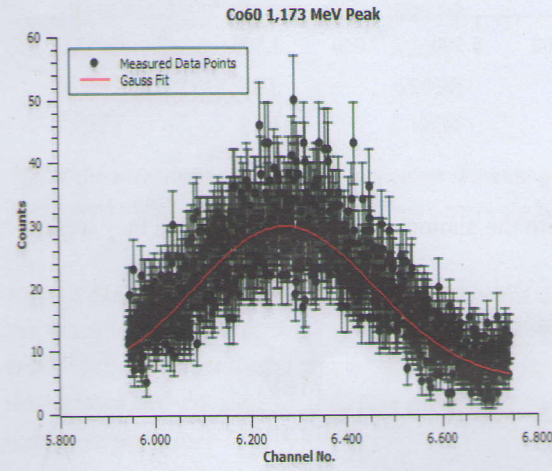
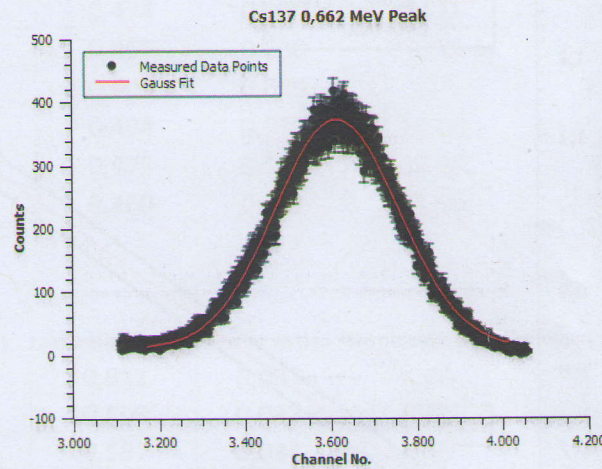
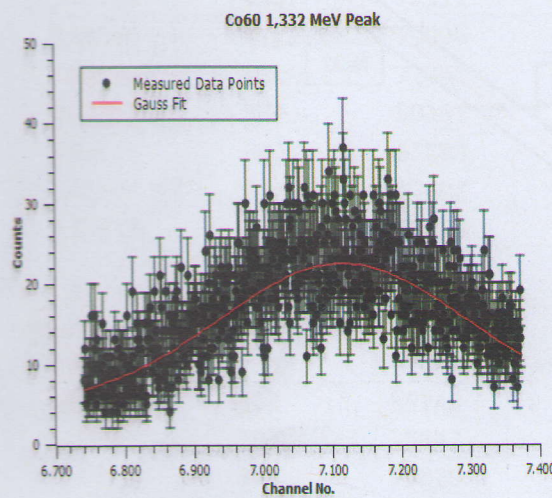
The calibration of the NaJ-Scintillator was done by recording the spectra of ^{60}Co (2 peaks at 1,332 MeV and 1,173 MeV respectively), ^{22}Na (1,275 MeV) and ^{137}Cs (0,662 MeV) by using the program (MAESTRO) that was preinstalled on the Pc in the working space. Every measurement was taken in a 120s time span. The FWHM of the peaks was used as measurement error. An oscilloscope was used to make sure the impulses detected were in the range that was set for the multichannel-analyzer. Else wise the registered peaks would have been cut off.

Following some exemplary pictures of the output given by the oscilloscope.



As the program MAESTRO was giving out absurdly small values for the FWHM for the NaJ-Scintillator measurement we decided to analyze the peaks of the spectra with an external program called SciDAVis.

Graphical Analysis of the Photopeaks via SciDAVis:



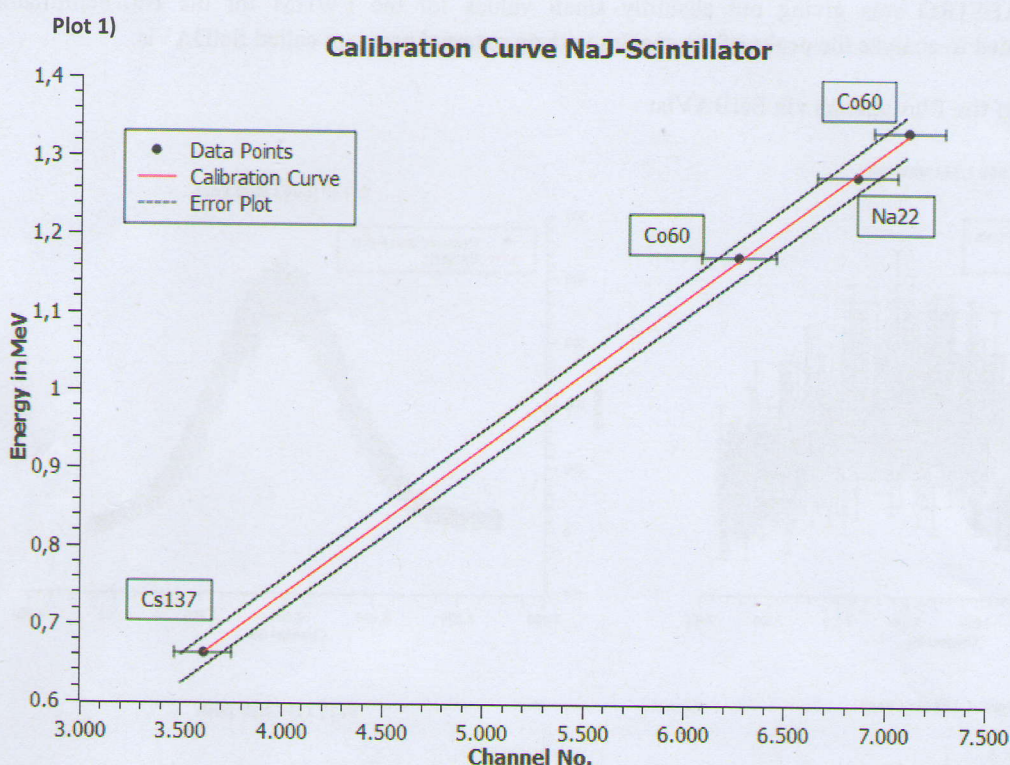
Unfortunately it was not possible to properly fit the photopeak of ^{22}Na as the source appears to have been too weak compared to the ^{60}Co and ^{137}Cs sources. Even though the peak is clearly visible the number of counts is relatively small in comparison. Additionally there is a great number of channels situated in the peak that did not register any counts at all explaining any programs difficulty to Gauss fit the data. This could have been avoided by measuring longer or downscaling the resolution of the multichannel-analyzer to around 500 channels instead of around 8000, which would have benefitted the measurements of the other elements as well.

Following data about the peaks was obtained via use of SciDAVis:

Table 1) Calibration Data for NaJ-Scintillator

	Channel of Photpeak Maximum	Channel Error (FWHM/2)	Energy in MeV
Cs137	3.613	143,5	0,662
Co60	6.271	187,88	1,173
Na22	6859*	200* (estimated)	1,275
Co60	7.115	177,5	1,332

*For ^{22}Na we chose to use the photopeak location calculated by MAESTRO and estimated the error a little bigger than for the other peaks as we couldn't analyse it properly)



For the graphical analysis the error of the energy values associated with the photopeaks were neglected, as they were much smaller than the channel errors.

The analysis gives us following calibration curve for the NaJ-Scintillator: (Plot 1)

$$E = (-0,027 \pm 0,012)\text{MeV} + (0,0001905 \pm 0,0000019) \frac{\text{MeV}}{\text{Channel}} * x$$

1.2 Measuring of Mass Attenuation Coefficients of different Absorber Materials:

To determine the mass attenuation coefficients of aluminum, copper and lead we used a stronger source of ^{60}Co . Therefore we marked a region of interest containing the 1,332 MeV photopeak. Now we put a number of little plates of the absorber material with a thickness of 2mm to 3mm in front of the radioactive source. We measured the number of events in our region of interest for each thickness of absorber material. Again our measurement time was 120s.

As error for the thickness of the absorber plates we estimated a value of 0,10mm. The error of the number of measured incidents in our region of interest is calculated as statistical error ($\Delta N = \sqrt{N}$)

Following data was obtained with Maestro:

Table 2.1)

Measurement Lead							
Gross area	error	Net area	error Net	ratio net/gross	error ratio	Thickness [mm]	error thickness
159312	399	75590	3072	0,474	0,031	3,00	0,10
133786	366	68004	2724	0,508	0,033	6,00	0,14
112660	336	59064	2460	0,524	0,036	9,00	0,17
94933	308	49123	2274	0,517	0,038	12,00	0,20
82247	287	44448	2066	0,540	0,041	14,50	0,22
73217	271	36095	2046	0,493	0,041	16,50	0,24

Table 2.2)

Measurement Aluminium							
Gross area	error	Net area	error Net	ratio net/gross	error ratio	Thickness [mm]	error thickness
172114	415	72311	3240	0,420	0,028	3,00	0,10
168566	411	79898	3093	0,474	0,030	6,00	0,14
160698	401	72560	3066	0,452	0,030	9,00	0,17
147708	384	60191	2928	0,407	0,029	12*	0,20
145925	382	63288	2916	0,434	0,030	15,00	0,22
142208	377	67607	2806	0,475	0,031	18,00	0,24
135917	369	62489	2781	0,460	0,031	21,00	0,26

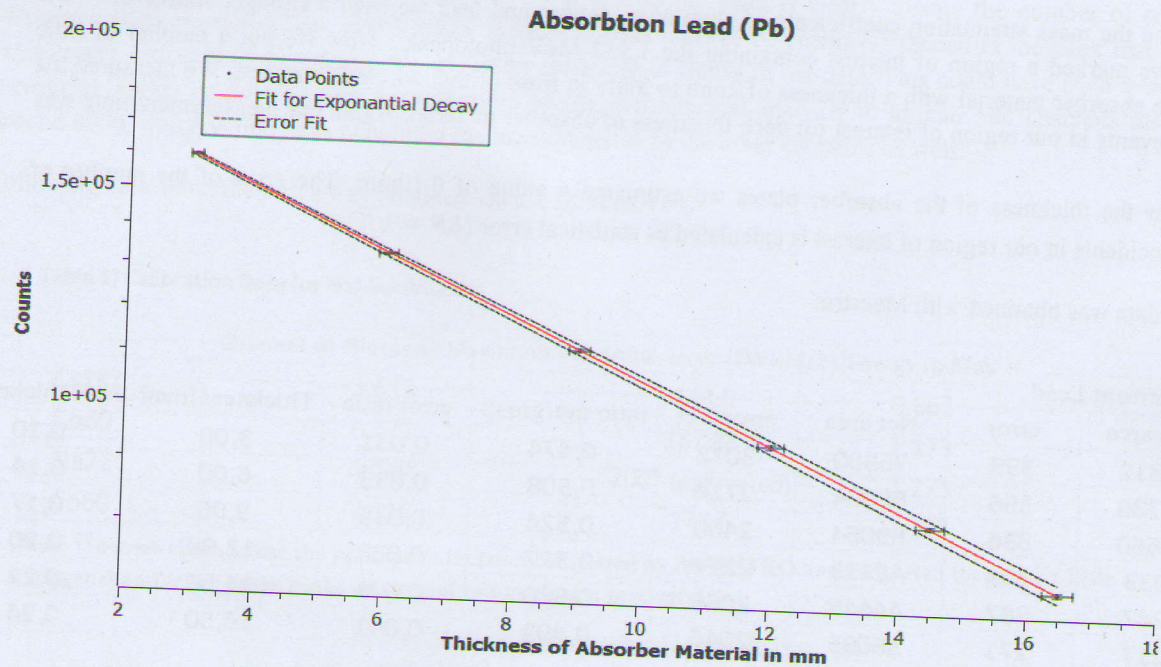
Table 2.3)

Measurement Copper							
Gross area	error	Net area	error Net	ratio net/gross	error ratio	Thickness [mm]	error thickness
167640	409	85740	3089	0,511	0,031	3,00	0,10
149636	387	75542	2938	0,505	0,032	6,00	0,14
141071	376	75820	2802	0,537	0,034	8,00	0,17
123561	352	65049	2698	0,526	0,036	11,00	0,20
109067	330	59529	2416	0,546	0,037	14,00	0,22
97290	312	47974	2420	0,493	0,037	17,00	0,24
85277	292	41498	2222	0,487	0,039	19,50	0,26
75077	274	34904	2092	0,465	0,040	22,00	0,28

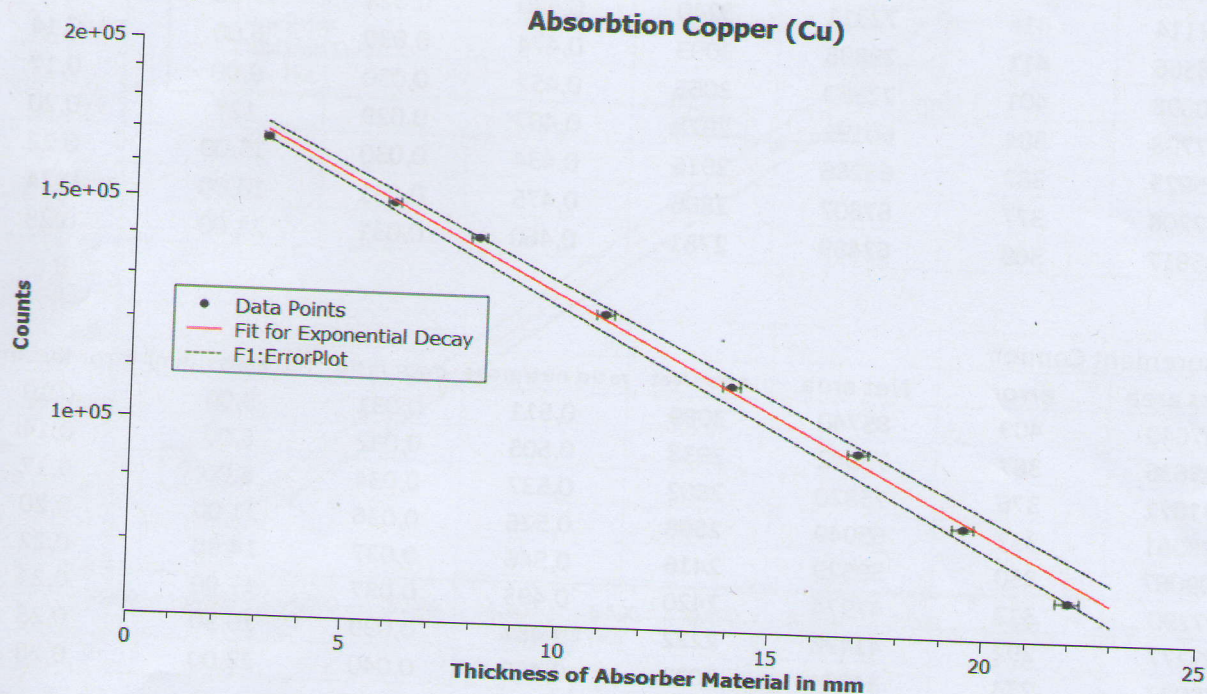
*For the measurement of Al we neglected the data point at 12mm thickness because the value did not fit the alignment of the other data points. There seems to have been a mistake during the measurement

As one can see in the tables 2.1) to 2.3) Maestro calculated two kinds of areas from the peak. The Gross area being the whole area in our region of interest, the Net area being supposed to be some kind of background noise. As both areas seem to undergo the same kind of decay as indicated by their somewhat stable ratios for changing absorber thicknesses we decided to only use the gross area for the determination of the mass absorption coefficients to minimize the error.

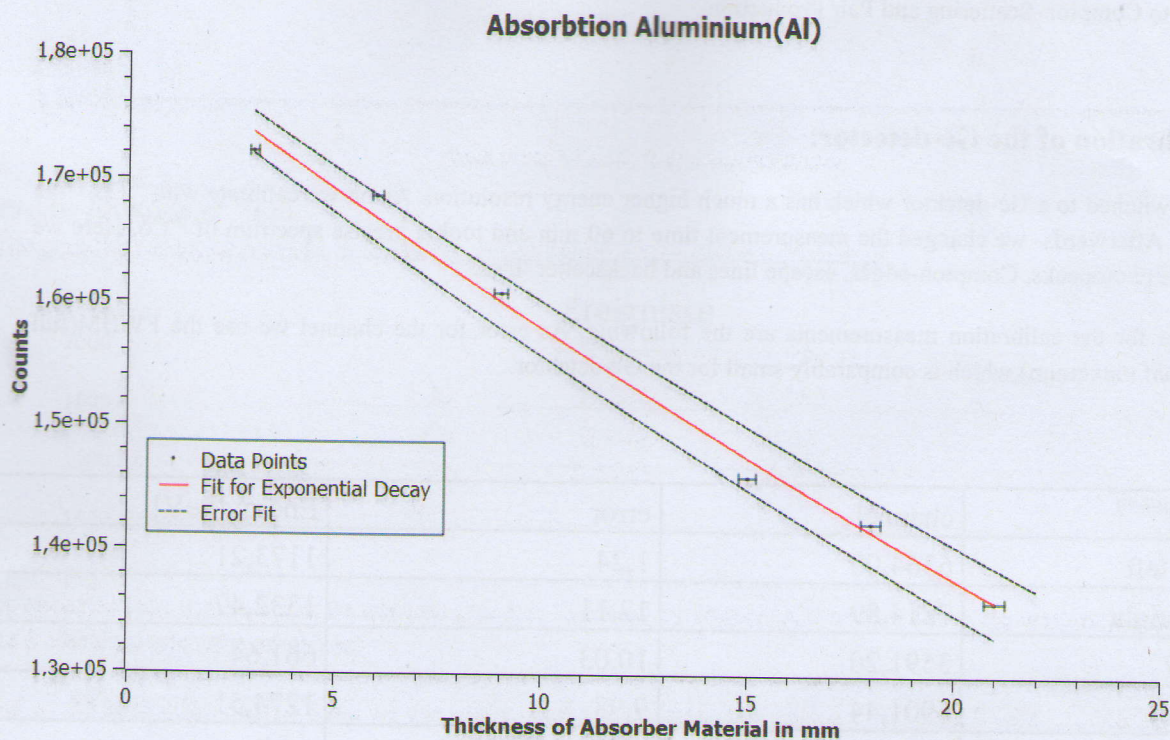
Plot 2.1)



Plot 2.2)



Plot 2.3)



The graphical analysis resulted in following values for the absorbtion coefficient μ :

	μ in 1/mm	$\Delta\mu$ in 1/mm
Al	0,1360	0,0062
Cu	0,409	0,011
Pb	0,5751	0,0010

As expected lead turned out to be the best absorber followed by copper. Aluminium being the weakest absorber of the 3 elements that were examined.

Out of the absorbtion coefficient μ we can easily calculate the mass attenuation coefficient $\frac{\mu}{\rho}$ with knowledge of the densities of our materials

$$\text{Lead(Pb): } \rho = 11,342 \text{ g/cm}^3$$

$$\text{Copper(Cu): } \rho = 8,92 \text{ g/cm}^3$$

$$\text{Aluminium(Al): } \rho = 2,7 \text{ g/cm}^3$$

	μ/ρ in cm^2/g	$\Delta(\mu/\rho)$ in cm^2/g
Al	0,0504	0,0023
Cu	0,046	0,0012
Pb	0,0507	0,000080

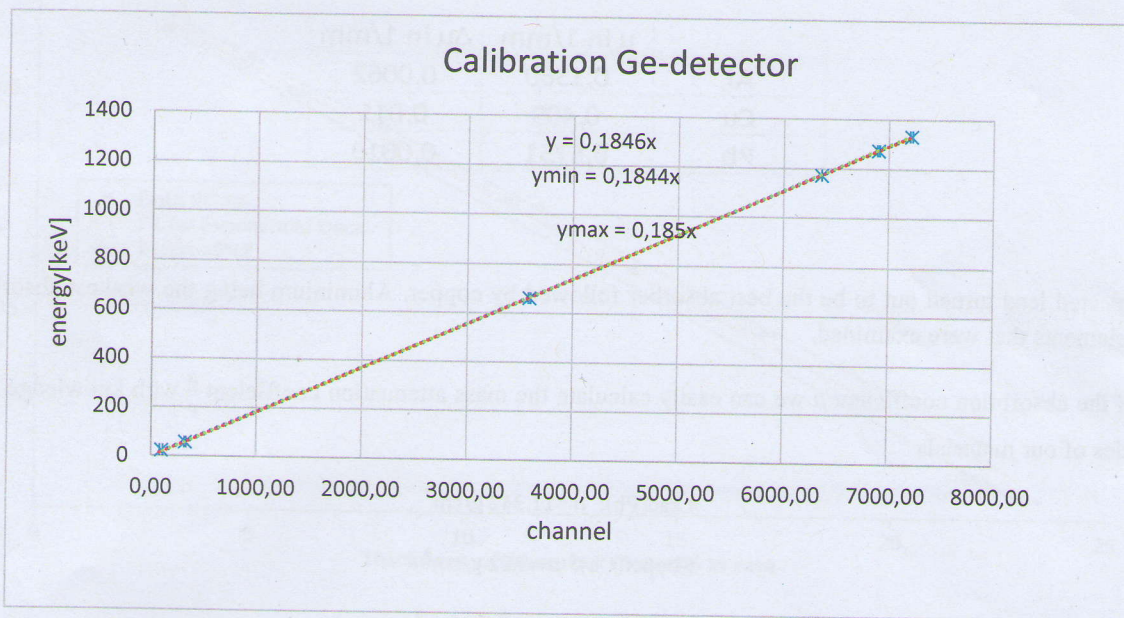
It appears that the mass attenuation coefficient is relatively independent of the absorber material in our energy range. This might be because the photoeffect which is highly material dependant loses importance in higher energy levels compared to Compton-Scattering and Pair Production

1.3 Calibration of the Ge-detector:

Now we switched to a Ge-detektor which has a much higher energy resolution. Again we calibrate with ^{60}Co , ^{22}Na and ^{137}Cs . Afterwards we changed the measurement time to 60 min and took a precise spectrum of ^{60}Co . Here we marked the photopeaks, Compton-edges, escape lines and backscatter lines.

Our results for the calibration measurements are the following. As error for the channel we use the FWHM(full width at half maximum),which is comparably small for the Ge-detektor.

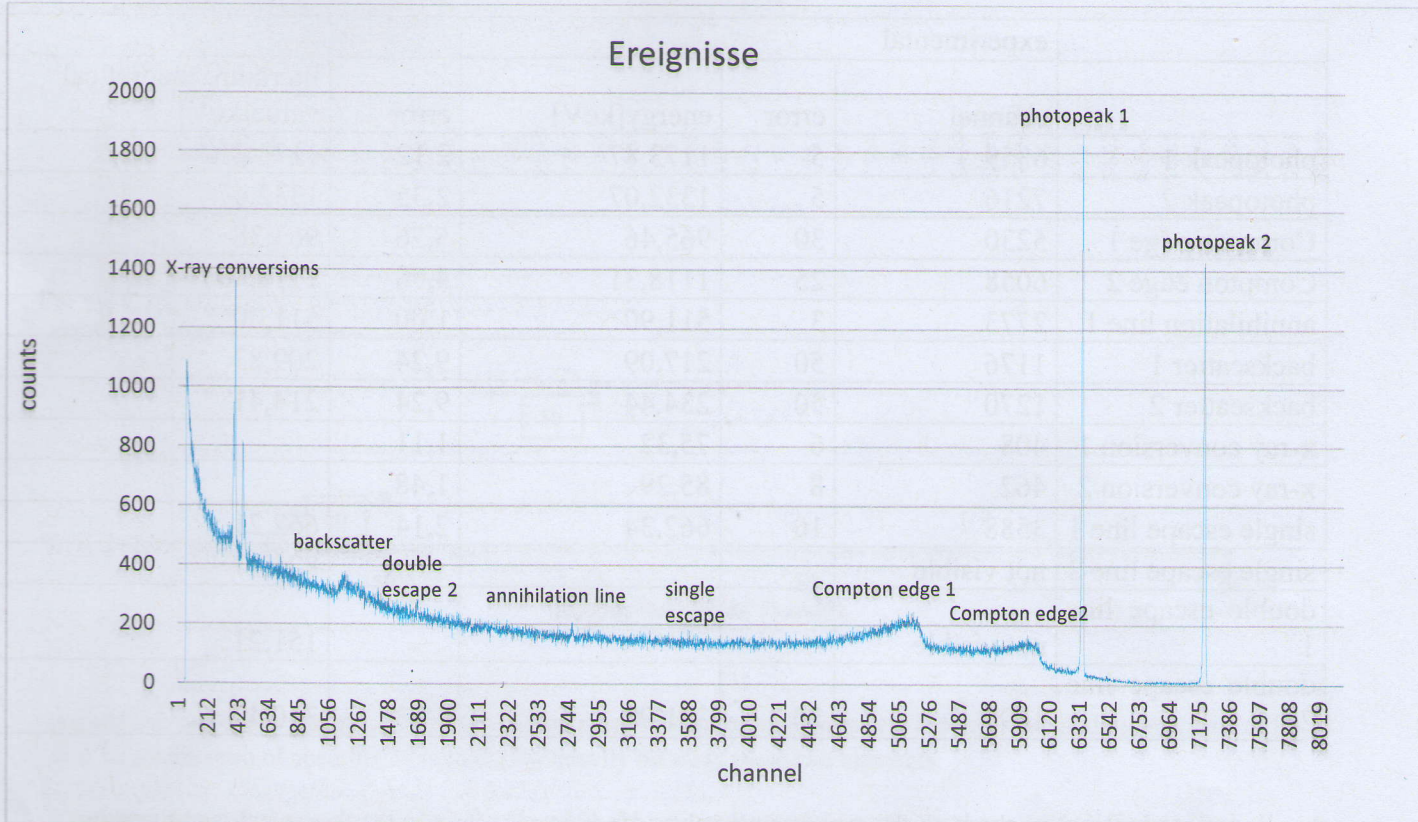
Peak	channel	error	Energy[keV]
Co60 left	6364,00	1,24	1173,21
Co60 right	7214,89	12,11	1332,47
Cs137	3591,20	10,03	661,64
Na22	6901,44	9,98	1274,51
Am241 right	324,06	7,34	59,58
Am241 left	96,85	15,34	26,35



As the errors for the channel are very small we have a very precise linear fit with the slope:

$$0,1846 \pm 0,0003 \frac{\text{keV}}{\text{Channel}}$$

Precise spectrum of ${}^{60}\text{Co}$:



For the Compton-effect we have the following relation:

$$E' = E - \frac{E}{1 + \frac{E}{m_e c^2} (1 - \cos \vartheta)}$$

With $\vartheta=180^\circ$ (maximum energy) we have

$$E' = E - \frac{E}{1 + \frac{2E}{m_e c^2}}$$

So we expect the Compton-edges at 963,38keV and 1318,06keV

The annihilation line is at $E = m_e c^2 = 511\text{keV}$, which is the rest mass of an electron/positron.

Then there are also the escape lines which are created by escaping electrons from pair production. They have the energy of the photo peak minus the energy of the annihilation. So we expect them at

$$1173\text{keV}-511\text{keV}/1022\text{keV} = 662\text{keV}/151\text{keV} \text{ and}$$

$$1332\text{keV}-511\text{keV}/1022\text{keV} = 821\text{keV}/310\text{keV}$$

The **backscatter lines** represent the energy that is transferred to the electrons via Compton effect. So we expect them at **963,38keV** and **1118,06keV**.

	experimental				
	channel	error	energy[keV]	error	literature/theoretical value[keV]
photopeak 1	6359	5	1173,87	2,12	1173,21
photopeak 2	7216	5	1332,07	2,35	1332,47
Compton edge 1	5230	30	965,46	5,76	963,38
Compton edge 2	6058	25	1118,31	4,96	1118,06
annihilation line 1	2773	3	511,90	1,00	511,00
backscatter 1	1176	50	217,09	9,24	209,83
backscatter 2	1270	50	234,44	9,24	214,41
x-ray conversion 1	408	6	75,32	1,11	
x-ray conversion 2	462	8	85,29	1,48	
single escape line 1	3588	10	662,34	2,14	662,21
single escape line 2	not visible				821,47
double escape line 1	not visible				151,21
double escape line 2	1690	20	311,97	3,73	310,47

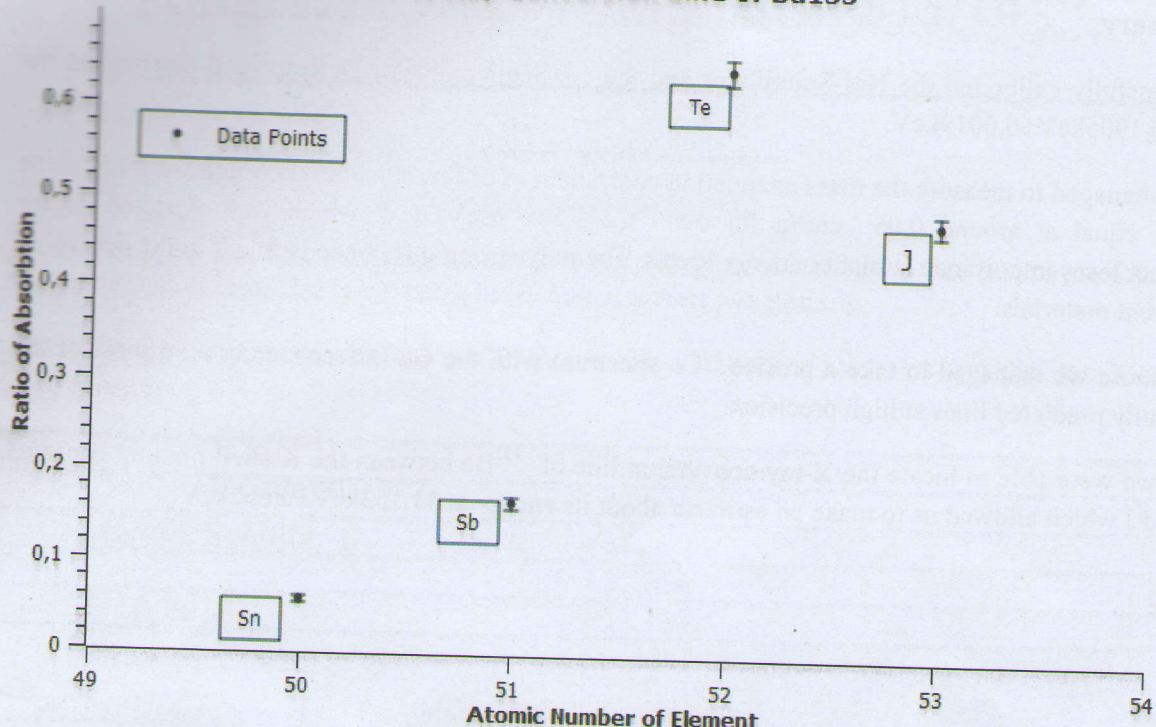
As you can see in the chart above all the experimental values are extremely close to the theoretical- and literature values. Some escape lines weren't visible but that may have changed if we used an even longer measurement time. The backscatter lines weren't easy to separate so we have relatively high error values (compared to the other values in the chart).

1.4 Determination of the x-ray conversion line by using critical absorption:

Finally we measure the spectrum of ^{133}Ba with the Ge-Detector and mark areas containing the X-ray-conversion peaks at channel 168 and the photopeak at channel 440 and read out the count rates for these. We repeated this with different absorbers with rising atomic numbers from 50 to 53 (namely Sn, Sb, Te and J) between the source and the detector. We then used the ratio between the conversion peak areas with absorbers and without to plot the absorbtion ratios against the atomic number of the elements used as absorbers. Again we only used the Gross area of the peaks given out by Maestro for reasons stated farther above.

atomic number	conversion peak area	error area	ratio of absorbtion	error of ratio
none	5490	74		
50(Sn)	309	18	0,0563	0,0033
51(Sb)	904	30	0,1647	0,0059
52(Te)	3.528	59	0,643	0,014
53(J)	2.617	51	0,477	0,011

X-Ray Conversion Line of Ba133



As one can see in our plot the critical absorption must be happening somewhere between the binding energies of Sb and Te, as the ratio of absorption is increasing heavily between these two elements.

To determine the x-ray conversion line at $\approx 30\text{keV}$ we used a number of absorbers with different K-shell binding energies:

Element	Binding energy[keV]
Sn	29,200
Sb	30,491
Te	31,814
J	33,169

As our line of interest is at about 30keV and our critical absorption is between Sb and Te the most important numbers are the binding energies of Sb ($30,491\text{ keV}$) and Te($31,814\text{ keV}$). So we may approximate the energy of that line with

$$E = \frac{30,491\text{keV} + 31,814\text{keV}}{2} = 31,153\text{keV}$$

Our error for this measurement is half of the distance between the two energies:

$$\Delta E = \frac{31,814\text{keV} - 30,491\text{keV}}{2} = 0,662\text{keV}$$

3. Summary

We successfully calibrated the NaJ-Scintillator and the Ge-Semiconductor-Detector and determined the slope to $0,1905\text{keV} \pm 0,0019\text{keV}$.

We then managed to measure the mass attenuation coefficient of different materials which we found to be relatively equal at around $0,05\text{ cm}^2/\text{g}$ for our ^{60}Co 1,332 MeV peak which was expected as the photoeffect loses importance at higher energy levels. The only strong difference is found in the density of the different materials.

Furthermore we managed to take a precise ^{60}Co spectrum with the Ge-Detector and found most of the theoretically predicted lines at high precision.

Finally we were able to locate the X-ray conversion line of ^{133}Ba between the K-shell binding energies of Te and J which allowed us to make an estimate about its energy at $31,153\text{keV} \pm 0,662\text{keV}$.